

# Journal of Materials Chemistry B

Accepted Manuscript



This is an *Accepted Manuscript*, which has been through the Royal Society of Chemistry peer review process and has been accepted for publication.

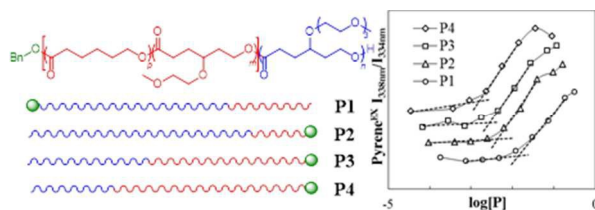
*Accepted Manuscripts* are published online shortly after acceptance, before technical editing, formatting and proof reading. Using this free service, authors can make their results available to the community, in citable form, before we publish the edited article. We will replace this *Accepted Manuscript* with the edited and formatted *Advance Article* as soon as it is available.

You can find more information about *Accepted Manuscripts* in the [Information for Authors](#).

Please note that technical editing may introduce minor changes to the text and/or graphics, which may alter content. The journal's standard [Terms & Conditions](#) and the [Ethical guidelines](#) still apply. In no event shall the Royal Society of Chemistry be held responsible for any errors or omissions in this *Accepted Manuscript* or any consequences arising from the use of any information it contains.

Graphical abstract

Manuscript ID TB-ART-12-2014-002016

*Fine-tuning thermoresponsive functional poly( $\epsilon$ -caprolactone)s to enhance micelle stability and drug loading*

New caprolactone-based  $\text{PME}_3\text{CL-}b\text{-P}(\text{ME}_1\text{CL-}co\text{-CL})$  terpolymers feature attractive properties including thermoresponsive behavior, biodegradable backbones, and enhanced micelle stability.

## Fine-tuning thermoresponsive functional poly( $\epsilon$ -caprolactone)s to enhance micelle stability and drug loading

Cite this: DOI: 10.1039/x0xx00000x

Received 00th January 2012,  
Accepted 00th January 2012

DOI: 10.1039/x0xx00000x

www.rsc.org/

Elizabeth A. Rainbolt,<sup>a</sup> Jason B. Miller,<sup>b</sup> Katherine E. Washington,<sup>a</sup> Suchithra A. Senevirathne,<sup>a</sup> Michael C. Biewer,<sup>a</sup> Daniel J. Siegwart,<sup>b,\*</sup> Mihaela C. Stefan<sup>a,\*</sup>

Block copolymers synthesized by the ring-opening polymerization of  $\gamma$ -2-[2-(2-methoxyethoxy)ethoxy]ethoxy- $\epsilon$ -caprolactone (ME<sub>3</sub>CL),  $\gamma$ -2-methoxyethoxy- $\epsilon$ -caprolactone (ME<sub>1</sub>CL), and  $\epsilon$ -caprolactone (CL) are reported. Previously, diblock copolymers of PME<sub>3</sub>CL-*b*-PME<sub>1</sub>CL displayed excellent thermoresponsive tunability (31 – 43 °C) and self-assembled into micelles with moderate thermodynamic stability. In this report, two strategies are employed to enhance thermodynamic stability of PME<sub>3</sub>CL/PME<sub>1</sub>CL-type block copolymer micelles while maintaining their attractive thermoresponsive qualities: modification of the end group position and alteration of hydrophobic block composition by using both ME<sub>1</sub>CL and CL. These new thermoresponsive amphiphilic block copolymers showed lower critical micelle concentration (CMC) values by one order of magnitude and formed thermodynamically stable micelles. Furthermore they demonstrated good biocompatibility and up to 4.97 wt % doxorubicin loading, more than double the amount loaded into the PME<sub>3</sub>CL-type polymeric micelles previously reported.

### Introduction

In the development of drug delivery systems, synthetic polymers offer versatility in terms of biocompatibility, self-assembly, and stimuli-responsive features.<sup>1–6</sup> Poly( $\epsilon$ -caprolactone)s are of particular interest due to their hydrolyzable backbones and array of properties attainable by attaching functional groups along the polymer chain.<sup>6–12</sup> Recently, by the ring-opening polymerization (ROP) of  $\gamma$ -2-[2-(2-methoxyethoxy)ethoxy]ethoxy- $\epsilon$ -caprolactone (ME<sub>3</sub>CL),  $\gamma$ -2-methoxyethoxy- $\epsilon$ -caprolactone (ME<sub>1</sub>CL), and other  $\gamma$ -substituted caprolactone (CL) monomers, amphiphilic block copolymers were synthesized and investigated for use as micellar vehicles for drug delivery by our group.<sup>3, 13–15</sup> PME<sub>3</sub>CL served as the hydrophilic segment and imparted lower critical solution temperature (LCST) behavior to the block copolymer in the form of a cloud point, the temperature at which a thermoresponsive polymer in water undergoes a coil-to-globular transition. For the hydrophobic segment, alkoxy-, benzyloxy-, and methoxyethoxy-substituted poly( $\epsilon$ -caprolactone)s were explored.<sup>3, 15</sup> By adjusting the hydrophilic/hydrophobic block ratios and/or the functional groups on the hydrophobic block, the LCST behavior could be tuned in the range of 31 – 44 °C.<sup>15</sup> Due to their combined thermoresponsive and biodegradable properties, this family of

copolymers constitutes a new direction in synthetic polymeric micelles for controlled drug delivery applications.

In a drug carrier application, micelle-forming block copolymers with LCST behavior above 37 °C would encapsulate drug molecules, infiltrate the body, and accumulate in solid tumors by the enhanced permeability and retention (EPR) effect.<sup>16</sup> Warming the micelles above the cloud point, by localized heating or mild hyperthermia would dehydrate the PME<sub>3</sub>CL shells, thusly deforming the micelles and triggering the release of their drug cargoes.<sup>14</sup> While the thermoresponsive properties of PME<sub>3</sub>CL-*b*-PME<sub>1</sub>CL displayed excellent tunability, their critical micelle concentrations (CMC) were moderate at best, and thus prompted the redesign of the polymer architecture.<sup>15</sup>

As documented in literature, the positioning of end groups can influence substantially the physical properties of polymers, such as self-assembly and LCST.<sup>17–22</sup> Typically, to reduce the CMC of an amphiphile—and thereby increase its thermodynamic stability—efforts are focused on lengthening the core-forming segment and/or reducing its hydrophilicity.<sup>23</sup> In the case of the PME<sub>3</sub>CL-*b*-PME<sub>1</sub>CL copolymers, the hydrophobic block was comprised of methoxyethoxy-functionalized caprolactone units. Block copolymers featuring ME<sub>1</sub>CL in the hydrophobic block were posited to enhance

micelles' drug loading capacity due to the possibility of hydrogen bonding with encapsulated anticancer drugs like doxorubicin (DOX). While ME<sub>1</sub>CL is less hydrophilic than ME<sub>3</sub>CL, its side units are more hydrophilic than an alkoxy-substituted caprolactone. However, the effects on drug encapsulation by incorporating unsubstituted caprolactone within the hydrophobic block alongside ME<sub>1</sub>CL had not been reported.

We hypothesized that improved micelle stability would result from self-assembled diblock copolymers in which: (1) the ROP initiator was relegated to the hydrophobic chain end, and (2) the core-forming block was a random copolymer of ME<sub>1</sub>CL and CL. Thus, a series of block copolymers containing CL, ME<sub>1</sub>CL, and ME<sub>3</sub>CL were synthesized by ring-opening polymerization and investigated for use as micellar drug carriers. Their cloud points, CMCs, micelle sizes and stabilities were examined. Preliminary biological studies were performed to probe the polymer cytotoxicity, drug loading, stability in serum-containing media, and micelle uptake by HeLa cells.

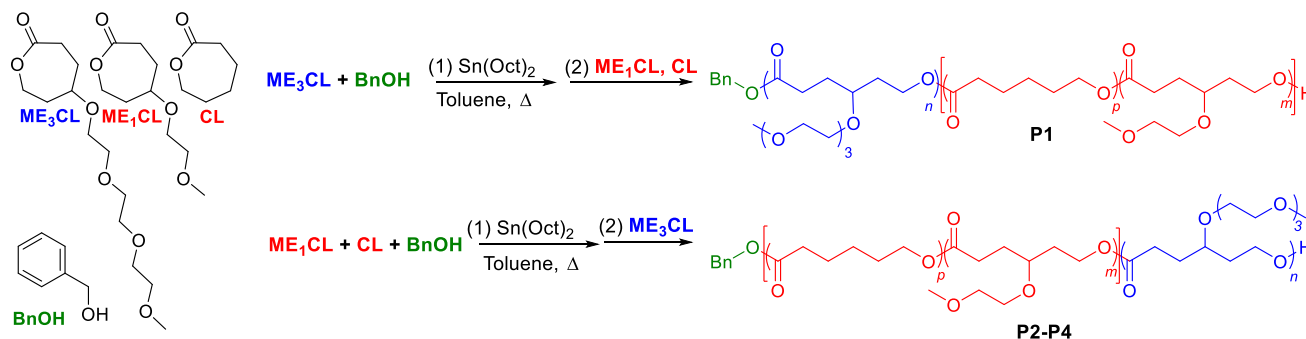
## Results and Discussion

In an effort to improve the micelle stability of PME<sub>3</sub>CL-*b*-PME<sub>1</sub>CL copolymers, unsubstituted  $\epsilon$ -caprolactone was incorporated into the hydrophobic block. It was hypothesized that different self-assembly behavior might result from a terpolymer in which the hydrophobic block was a random copolymer of ME<sub>1</sub>CL and CL. First, an experiment was performed to see if in a copolymerization of ME<sub>1</sub>CL and CL, one monomer would be more active than the other, and a

gradient copolymer would be formed. Briefly, equimolar quantities of both ME<sub>1</sub>CL and CL were mixed together and subjected to ring-opening polymerization with stannous(II) 2-ethylhexanoate and benzyl alcohol as initiator. Samples were taken periodically, and shown in Fig. S1 are <sup>1</sup>H NMR spectra of the raw polymer at time points from 5 to 60 minutes. Chemical shifts of the methylene protons adjacent to oxygen in the cyclic ME<sub>1</sub>CL and CL monomers differ from those of the caprolactone units incorporated into the polymer. Because those signals do not overlap, the number of repeat units of each CL and ME<sub>1</sub>CL ( $\delta_{\text{H}} = 4.06$  ppm, 4.17 ppm) could be calculated by integration and comparison to the integration of the benzylic protons of the initiator ( $\delta_{\text{H}} = 5.11$  ppm). As shown in Table S1, the units of ME<sub>1</sub>CL and CL per chain at the given time points are comparable.

### Block copolymer synthesis

With evidence pointing towards random copolymerization of ME<sub>1</sub>CL and CL rather than a gradient, four block copolymers (**P1** – **P4**) were synthesized with hydrophobic blocks comprised of randomly incorporated ME<sub>1</sub>CL and CL units. As reported in our prior publication, a block copolymer with 76 mol% ME<sub>3</sub>CL and 24 mol% ME<sub>1</sub>CL, displayed a cloud point of 38.5 °C.<sup>15</sup> Thus a similar hydrophilic : hydrophobic molar ratio for **P1** was targeted.<sup>15</sup> Briefly, ME<sub>3</sub>CL was subjected to tin-catalyzed ROP and upon its consumption, ME<sub>1</sub>CL and CL were added simultaneously to generate polymer **P1**, as illustrated in Scheme 1. Polymers **P2** – **P4** were prepared by the copolymerization of ME<sub>1</sub>CL and CL, followed by addition of the ME<sub>3</sub>CL to generate the hydrophilic block. For **P2** – **P4**, the benzyl group from the initiator is situated at



**Scheme 1.** Ring-opening polymerization (ROP) of  $\gamma$ -2-[2-(2-methoxyethoxy)ethoxy]ethoxy- $\epsilon$ -caprolactone (ME<sub>3</sub>CL),  $\gamma$ -2-methoxyethoxy- $\epsilon$ -caprolactone (ME<sub>1</sub>CL), and  $\epsilon$ -caprolactone (CL), using benzyl alcohol initiator (BnOH) and stannous(II) 2-ethylhexanoate catalyst to generate amphiphilic block copolymers **P1** – **P4**.

**Table 1.** Summary of amphiphilic block copolymers **P1** – **P4**

| Polymer   | $M_n^{\text{NMR}^a}$<br>(kg mol <sup>-1</sup> ) | $M_n^{\text{SEC}^b}$<br>(kg mol <sup>-1</sup> ) | PDI <sup>b</sup> | ME <sub>3</sub> CL <sup>a</sup><br>(mol %) | ME <sub>1</sub> CL <sup>a</sup><br>(mol %) | CL <sup>a</sup><br>(mol %) | CMC <sup>c</sup><br>(mg mL <sup>-1</sup> ) | LCST <sup>d</sup><br>(°C) | $D_h^e$<br>(nm) | Micelle<br>dispersity <sup>e</sup> |
|-----------|---|---|------------------|--|--|----------------------------|--|---------------------------|-----------------|------------------------------------|
| <b>P1</b> | 33.3  | 10.9  | 2.01             | 71   | 13   | 16                         | 13.87 x 10 <sup>-3</sup>                   | 44.3                      | 55.4 ± 1.6      | 0.320                              |
| <b>P2</b> | 47.2  | 7.0   | 2.12             | 79   | 12   | 9                          | 4.39 x 10 <sup>-3</sup>                    | 54.2                      | 38.5 ± 0.2      | 0.363                              |
| <b>P3</b> | 40.3  | 4.4   | 1.95             | 42   | 51   | 7                          | 3.21 x 10 <sup>-3</sup>                    | 40.8                      | 79.8 ± 0.6      | 0.108                              |
| <b>P4</b> | 17.0  | 5.7   | 1.76             | 31   | 53   | 16                         | 1.34 x 10 <sup>-3</sup>                    | 29.9                      | 106.1 ± 0.5     | 0.144                              |

<sup>a</sup> Calculated from <sup>1</sup>H NMR, spectra shown in ESI Fig. S2 - Fig. S5. <sup>b</sup> Estimated by size exclusion chromatography (SEC), traces shown in ESI Fig. S6. <sup>c</sup> Critical micelle concentration (CMC) was measured using pyrene as a probe. <sup>d</sup> Cloud point was determined by monitoring the change in % transmittance at 600 nm of aqueous polymer solution as a function of temperature. <sup>e</sup> Hydrodynamic diameter and micelle dispersity was measured by DLS.

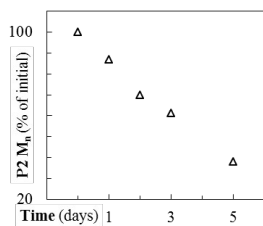


**Fig. 1.** Demonstration of degradability of **P2**: decrease in  $M_n$  as a function of time, performed in PBS solution (pH 7.4) at 37 °C over the course of 5 days.

the hydrophobic chain end, as shown in Scheme 1. This change in block copolymer structure from **P1** to **P2** – **P4** was hypothesized to facilitate the self-assembly of stable micelles.

The  $^1\text{H}$  NMR spectra for **P1** – **P4** are shown in Figs. S2 – S5, and the polymer compositions are summarized in Table 1. The  $M_n$  acquired from size exclusion chromatography (SEC) was much lower than the one calculated by  $^1\text{H}$  NMR. In SEC, samples are eluted according to hydrodynamic volume, which does not necessarily correlate with molecular weight. Typically the SEC is calibrated with poly(styrene) standards. Two polymers of comparable molecular weight may have very different hydrodynamic volumes depending on their makeup, and as a result, SEC has been shown to underestimate  $M_n$  in some cases.<sup>3, 24, 25</sup> In the case of terpolymers **P1** – **P4**, the SEC traces show monomodal distributions, indicating the formation of block copolymers upon the addition of the second portion of monomer(s) (Fig. S6). A more accurate picture of molecular weight is calculated from  $^1\text{H}$  NMR by comparing the integration of the benzylic protons on the end group to that of protons in the repeat units, as described above for the  $\text{ME}_1\text{CL}/\text{CL}$  random copolymerization.

The terpolymers were expected to degrade over time in phosphate buffered saline (PBS) due to the hydrolysis of their polyester backbones. With the highest  $M_n$  of the terpolymers, **P2** was selected to demonstrate the terpolymers' degradability in simulated physiological conditions, i.e. 37 °C, pH 7.4 PBS. As shown in Fig. 1, over the course of five days in the buffer,

the molecular weight decreased by more than 60%.

### Self-assembly and thermoresponsive behavior

Critical micelle concentration (CMC) was measured using the hydrophobic fluorescent molecule, pyrene, as a probe.<sup>13, 15</sup> **P1** self-assembled into micelles in aqueous media above a concentration of  $1.39 \times 10^{-2} \text{ mg mL}^{-1}$  (Fig. 2). The CMC is in line with previously reported values,<sup>14, 15</sup> however, since improved thermodynamic stability was a primary objective in this study, **P2** – **P4** were synthesized differently than **P1** so that the benzyloxy from the initiator would be on the hydrophobic end of the polymer chain. This small change in backbone structure yielded the desired effect, evidenced in the lower CMC value of **P2**,  $4.39 \times 10^{-3} \text{ mg mL}^{-1}$  (Fig. 2 (e)). As the length of the hydrophobic block increased (Fig. 2 (f)), the CMC decreased to  $1.34 \times 10^{-3} \text{ mg mL}^{-1}$  for **P4**, indicating improved thermodynamic stability by one order of magnitude over **P1**. Also observed was reduced CMC when the benzyl group from the initiator was on the end of the hydrophobic block (as in **P2**, **P3**, and **P4**) rather than the on the hydrophilic end (as in **P1**). Furthermore, the block terpolymers with hydrophobic blocks composed of  $\text{PME}_1\text{CL-co-PCL}$  (**P1** – **P4**,  $\text{CMC} \sim 10^{-3} \text{ mg mL}^{-1}$ ) self-assembled into more stable micelles rather than those with just  $\text{PME}_1\text{CL}$  ( $\text{CMC} \sim 10^{-2} \text{ mg mL}^{-1}$ ).<sup>15</sup>

Due to the  $\text{PME}_3\text{CL}$  hydrophilic block, thermoresponsive properties were expected for each terpolymer. **P1** – **P4** all displayed LCST behavior, with cloud point decreasing as the mol % hydrophilic block decreased. This trend is in agreement with the one observed in the  $\text{PME}_3\text{CL-}b\text{-PME}_1\text{CL}$  diblock copolymers previously studied.<sup>15</sup> The cloud point for **P1** with 71 mol %  $\text{ME}_3\text{CL}$  was 44.3 °C; however, LCST behavior at lower temperature between 34.3 and 38.5 °C was expected based on the thermal properties of the diblock copolymers with 60 - 75 mol %  $\text{ME}_3\text{CL}$  content.<sup>15</sup> Thus, polymers with a hydrophobic block comprised of CL and  $\text{ME}_1\text{CL}$  have cloud points higher than polymers with hydrophobic blocks of  $\text{ME}_1\text{CL}$  alone. Regardless of the CL effect on LCST, **P1** – **P4**, with varying hydrophilic to hydrophobic block ratios, displayed LCST behavior between 30 - 54 °C, shown in Fig. 3 (a – d).

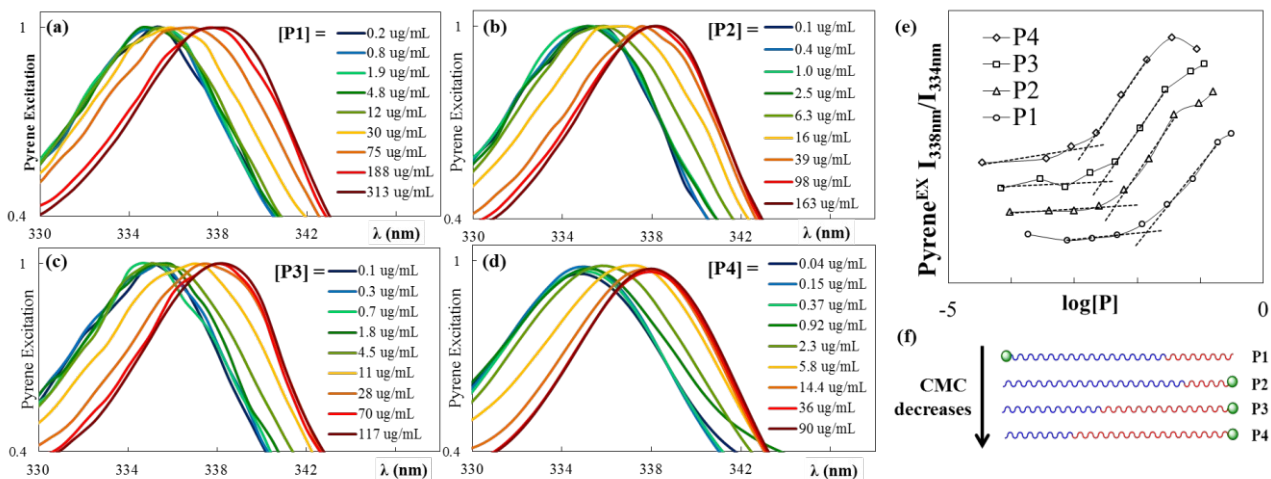


**Fig. 2.** CMC determination for **P1** – **P4**, (a – d), change in pyrene fluorescence vs. polymer concentration; (e) overlay of CMC data from **P1** – **P4**; (f) trend in CMC values for **P1** – **P4**, the green dot represents benzyloxy end group, blue represents hydrophilic block ( $\text{PME}_3\text{CL}$ ) and red represents hydrophobic block ( $\text{PME}_1\text{CL-co-PCL}$ ).

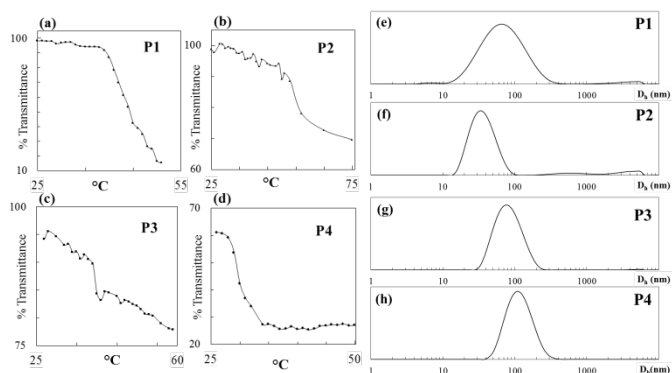


**Fig. 3.** LCST investigation for **P1** – **P4** (a – d), percent transmittance drops sharply upon heating above cloud point; DLS estimation of hydrodynamic diameters of empty micelles **P1** – **P4** (e – h).

The hydrodynamic diameters ( $D_h$ ) of the micelles formed by **P1** – **P4** ranged from 38 – 106 nm as estimated by DLS, shown in Fig. 3 (e – h). The target size for these micelles as drug carriers is in the range of 10 – 200 nm so as to exploit the EPR effect.<sup>26, 27</sup> The hydrodynamic diameter of empty micelles prepared from **P1**, **P2**, **P3**, and **P4** were about 55 nm, 39 nm, 80 nm, and 106 nm respectively, with micelle dispersity indices of 0.320, 0.363, 0.108, and 0.144. While the four sets of micelles closely match the targeted 10 – 200 nm window, the micelles from **P3** and **P4** were substantially more uniform than those of **P1** and **P2**, as indicated by their dispersity values of less than 0.200. This favorably low dispersity of the **P3** and **P4** micelles was attributed to their reduced CMC and relatively larger hydrophobic block lengths.

#### Doxorubicin encapsulation

One of the challenges in developing polymeric micellar drug delivery systems is low drug loading capacity.<sup>1, 28</sup> Previously reported  $\text{PME}_3\text{CL-}b\text{-poly}(\gamma\text{-alkoxy-CL})$  copolymers achieved 1 – 2.4 wt% doxorubicin (DOX) loading.<sup>3, 14</sup> To better encapsulate anticancer drug DOX, **P1** – **P4** were designed with  $\text{ME}_1\text{CL}$  units in the hydrophobic block to provide sites with which DOX may noncovalently interact. Drug loaded micelles were prepared with a polymer : drug feed weight ratio of 10:1. The encapsulation efficiency (wt % EE) and drug loading capacity (wt % LC) were calculated using the equations below.

$$\text{wt \% EE} = \frac{\text{wt of encapsulated DOX}}{\text{wt of total DOX added}} \times 100$$

$$\text{wt \% LC} = \frac{\text{wt of encapsulated DOX}}{\text{wt of polymer}} \times 100$$

**Table 2.** DOX-loaded terpolymer micelles

| Polymer                  | $D_h^a$ (nm) | Micelle dispersity <sup>a</sup> | EE (wt %) | LC (wt %) |
|--------------------------|--------------|---------------------------------|-----------|-----------|
| <b>P1</b> <sup>DOX</sup> | 177.9 ± 15   | 0.429                           | 49.7      | 4.97      |
| <b>P2</b> <sup>DOX</sup> | 141.3 ± 0.8  | 0.182                           | 44.8      | 4.48      |
| <b>P3</b> <sup>DOX</sup> | 199.9 ± 1.7  | 0.153                           | 30.9      | 3.09      |
| <b>P4</b> <sup>DOX</sup> | 272.3 ± 2.4  | 0.178                           | 34.4      | 3.44      |

<sup>a</sup>Determined by DLS.

The drug-loaded micelles were prepared by dialysis as described in the Experimental section. As summarized in Table 2, DOX loading capacity ranged from 3.09 wt % for **P3** up to 4.97 wt % for **P1**. At nearly 5 wt % loading, **P1** demonstrated a sizeable increase in doxorubicin loading over the previously reported  $\text{PME}_3\text{CL-}b\text{-poly}(\gamma\text{-ethoxy-CL})$  with only 2 wt % DOX loading.<sup>3</sup> This substantial increase was attributed to favorable noncovalent interactions between DOX and the methoxyethoxy pendant groups on the hydrophobic block. The molar ratio of  $\text{ME}_1\text{CL}$  to CL in the hydrophobic block also may have affected the loading capacity. As the mol % of CL increased relative to mol %  $\text{ME}_1\text{CL}$  in the order of **P3** < **P4** < **P2** < **P1**, so did the % LC. A higher incorporation of CL may increase the void volume in the micelle core, and thereby allow a greater quantity of DOX to be encapsulated.<sup>3</sup>

The **P1**<sup>DOX</sup> through **P4**<sup>DOX</sup> micelle sizes were determined by DLS and are summarized in Fig. 4. With the exception of **P1**<sup>DOX</sup>, the DOX-micelles displayed narrow polydispersities by DLS, indicating highly uniform micelles. The DOX-loaded micelles exhibited hydrodynamic diameters more than double those of the empty micelles (Fig. S7). A marked change in size from empty to loaded micelles has been documented in several reports, but **P1**<sup>DOX</sup>, **P2**<sup>DOX</sup>, and **P3**<sup>DOX</sup> micelles still fall within the upper range of sizes appropriate for micellar drug carriers.<sup>26, 29-31</sup> The larger  $D_h$  for loaded micelles also was observed by transmission electron microscopy, shown in Fig. S8.

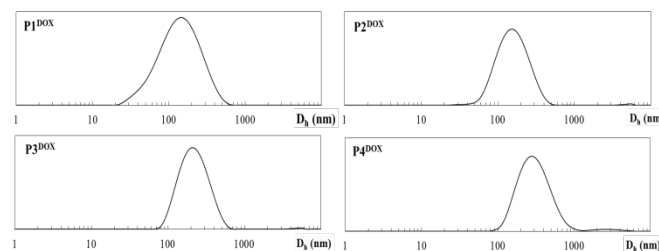


**Fig. 4.** DLS measurements: hydrodynamic diameters ( $D_h$ ) of DOX-loaded micelles of **P1** – **P4**.

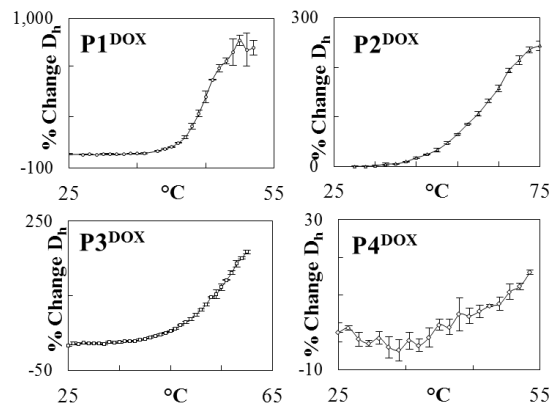


**Fig. 5.** Temperature-induced change in size of DOX-loaded micelles plotted as % change in  $D_h$  vs. temperature for **P1** – **P4**.

The thermoresponsive behavior of the DOX-loaded micelles is illustrated in Fig. 5. Plotted is the % increase in  $D_h$  as a function of temperature; each point represents the mean of three runs with vertical error bars signifying one standard deviation. As the suspensions were heated to above the polymers' cloud points, the apparent  $D_h$  increased markedly. This was attributed to the dehydration of the micelles'  $\text{PME}_3\text{CL}$ -based shells and subsequent aggregation of the deformed micelles and chains.

### Investigation of biocompatibility and cell studies

Micelles of **P3**, displaying LCST behavior closest to but greater than  $37^\circ\text{C}$ , were prepared and investigated for cytotoxicity, stability in serum-containing media, and cellular uptake using HeLa cells. Biocompatibility was examined by standard assay in which MTT, a yellow tetrazolium dye, is reduced by mitochondrial reductase in living cells to generate a purple formazan dye. The absorbance due to formazan in the micelle-treated cells was normalized to that of the control cells without micelle treatment, and was proportional to the amount of living cells. The empty micelles demonstrated no inherent cytotoxicity at dosages up to  $40\ \mu\text{g/mL}$ , and only contributed to a small reduction in cell viability at  $80\ \mu\text{g/mL}$  (Fig. 6 (a)).

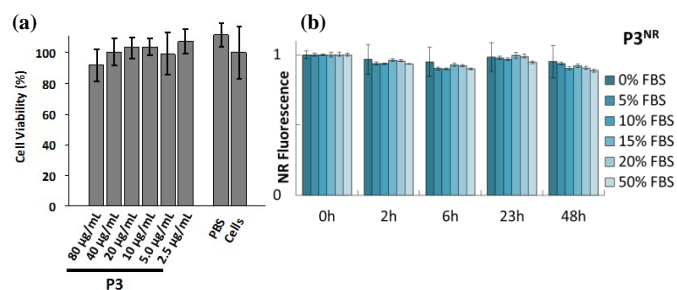


**Fig. 6.** (a) Biocompatibility of empty polymer micelles **P3**; cell viability determined by MTT assay; (b) Micelle stability of NR-loaded polymer micelles **P3<sup>NR</sup>** in serum-containing media.

PBS and fetal bovine serum (FBS) were used to test micelle stability by incubating Nile Red-loaded micelles **P3<sup>NR</sup>** in FBS (0 to 50 vol % in PBS) and monitoring changes in Nile Red (NR) fluorescence, as described in the experimental section. NR is a hydrophobic molecule which most strongly fluoresces in hydrophobic environments (e.g. a micelle core).<sup>32</sup> Should the micelle disassemble, NR would be exposed to the aqueous environment and its emission intensity would drop dramatically. For **P3<sup>NR</sup>**, no significant decrease in NR fluorescence was observed at any concentration of FBS during a 48 hour period, indicating the micelles were not destabilized by the protein media. The data is shown in Fig. 6 (b), where NR fluorescence is normalized to the initial intensity at  $t = 0$  hours.

To confirm their potential utility in biomedical applications **P3<sup>DOX</sup>** micelles were added to human cervical cancer cells (HeLa) and incubated at  $37^\circ\text{C}$  for 4 hours. The growth media was changed and the cells were incubated at  $37^\circ\text{C}$  for an additional 24 hours. Following incubation, the cells were washed and stained with DAPI so that the cell nuclei could be visualized by fluorescence microscopy, shown in Fig. 7 and Fig. S9. The red DOX signal appeared to be throughout the cell

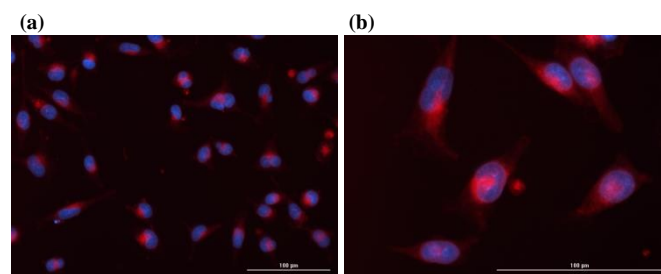


**Fig. 7.** Fluorescence microscopy images of HeLa cells after treatment with **P3<sup>DOX</sup>** micelles at (a) 20x magnification, and (b) 40x magnification; DOX shown in red, stained HeLa cell nuclei shown in blue; scale bars represent  $100\ \mu\text{m}$ .

cytoplasm, which suggested that the **P3<sup>DOX</sup>** micelles were internalized successfully by the HeLa cells.

## Experimental

### Materials

Nile Red (NR) was purchased from Chem-Impex International, Inc. Doxorubicin hydrochloride ( $\text{DOX}\cdot\text{HCl}$ , 99%) was purchased from AvaChem Scientific. All other commercial chemicals were purchased from Sigma-Aldrich Co. and were used without further purification unless otherwise noted. Benzyl alcohol and stannous (II) 2-ethylhexanoate were purified by vacuum distillation prior to use. All polymerization reactions were conducted under purified nitrogen. The polymerization glassware and syringes were dried at  $120^\circ\text{C}$  for at least 24 hours and then were cooled under nitrogen before use.

### Analysis

$^1\text{H}$  NMR spectra of the synthesized monomers and polymers were recorded on a Bruker AVANCE III 500 MHz NMR instrument at  $25^\circ\text{C}$  in  $\text{CDCl}_3$ .  $^1\text{H}$  NMR data are reported in parts per million as chemical shift relative to tetramethylsilane (TMS) as the internal standard. GC/MS was performed on an Agilent 6890-5973 GC/MS workstation. Polydispersity indices of the synthesized polymers were measured by size exclusion chromatography (SEC) analysis on a Viscotek VE 3580 system equipped with Viscogel columns (GMHHR-M), connected to a refractive index (RI) detectors. GPC (SEC) solvent/sample module (GPCmax) was used with HPLC grade THF as the eluent, and calibration was based on polystyrene standards. An Agilent UV/Vis spectrophotometer was employed for LCST measurements (% transmittance) and DOX loading determination (absorbance), described below. TEM imaging of the DOX-loaded micelles was performed on a Tecnai G2 Spirit Biotwin microscope by FEI and images were analyzed using ImageJ software. Samples were prepared by treating copper mesh grid with  $1\ \text{mg/mL}$  aqueous micelle solution for 2 minutes, followed by staining with 1% phosphotungstic acid for 30 seconds.

### Synthetic procedures

Monomers  $\gamma$ -2-methoxyethoxy- $\epsilon$ -caprolactone ( $\text{ME}_1\text{CL}$ ), and  $\text{ME}_3\text{CL}$  were synthesized according to previously described procedures.<sup>13, 15</sup>

**Synthesis of terpolymer P1 from  $\text{ME}_3\text{CL}$ ,  $\text{ME}_1\text{CL}$ , and CL.** A molar ratio of  $\text{ME}_3\text{CL} : \text{ME}_1\text{CL} : \text{CL} : \text{initiator} = 150 : 25 : 25 : 1$  was employed for **P1**. To an oven-dried 10 mL Schlenk flask,  $\text{ME}_3\text{CL}$  (0.48 g, 1.7 mmol) was introduced. The flask was placed under vacuum, and after an hour of pumping down, the vacuum in the Schlenk flask was cancelled with nitrogen. A thermostat-controlled oil bath was heated to 110 °C. A stock solution of benzyl alcohol (BnOH) containing 12.5 mg/mL in dry toluene was prepared and 0.1 mL BnOH stock solution (0.016 mmol BnOH) was loaded into a syringe. A solution of stannous(II) 2-ethylhexanoate (also known as tin octanoate,  $\text{Sn}(\text{Oct})_2$ ) containing 47 mg/mL in dry toluene was prepared and 0.1 mL  $\text{Sn}(\text{Oct})_2$  was loaded into a syringe. Promptly, the catalyst and initiator solutions were added to the flask, which was immediately lowered into the oil bath. In a clean scintillation vial,  $\text{ME}_1\text{CL}$  (0.055 g, 0.29 mmol) was combined with CL (0.033 g, 0.29 mmol), and placed under vacuum for 2 hours. The sample was monitored and analyzed by GC/MS and  $^1\text{H}$  NMR to check for residual monomer. Upon consumption of the  $\text{ME}_3\text{CL}$  (about 4 hours reaction time), the  $\text{ME}_1\text{CL}/\text{CL}$  mixture was dissolved in 0.2 mL toluene, and then added to the reaction vessel, which continued to stir at 110 °C. Samples were analyzed by GC/MS and  $^1\text{H}$  NMR to check for residual  $\text{ME}_1\text{CL}$  and CL monomers. Once no sign of monomer remained (about 8 hours total reaction time), the reaction mixture was removed from heat and dissolved in 2 mL THF, and then was poured into a beaker containing hexane, where it crashed out. The polymer was filtered and dried under vacuum, then analyzed by  $^1\text{H}$  NMR and SEC.  $M_n^{\text{NMR}} = 33.3 \text{ kg mol}^{-1}$ ,  $M_n^{\text{SEC}} = 10.9 \text{ kg mol}^{-1}$ ,  $\text{PDI}^{\text{SEC}} = 2.01$ .  $^1\text{H}$  NMR (500 MHz,  $\text{CDCl}_3$ ):  $\delta_{\text{H}}$  1.38 (dd, 0.34H), 1.65 (m, 0.68H) 1.82 (m, 4.3H), 2.30 (t, 0.33H), 2.39 (t, 1.9H), 3.36 (s, 2.9H), 3.59 (m, 12.4H), 4.06 (t, 0.33H), 4.17 (t, 2.0H), 5.11 (s, 0.016H).

**Synthesis of terpolymer P2.** A molar ratio of  $\text{ME}_3\text{CL} : \text{ME}_1\text{CL} : \text{CL} : \text{initiator} = 150 : 25 : 25 : 1$  was employed for **P2**. To an oven-dried 10 mL Schlenk flask,  $\text{ME}_1\text{CL}$  (0.055 g, 0.29 mmol) and CL (0.033 g, 0.29 mmol) were introduced. The flask was placed under vacuum, and after an hour of pumping down, the vacuum in the Schlenk flask was cancelled with nitrogen. A thermostat-controlled oil bath was heated to 110 °C. A stock solution of BnOH containing 12.5 mg/mL in dry toluene was prepared and 0.1 mL BnOH stock solution (0.016 mmol BnOH) was loaded into a syringe. A solution of tin ethylhexanoate ( $\text{Sn}(\text{Oct})_2$ ) containing 47 mg/mL in dry toluene was prepared and 0.1 mL  $\text{Sn}(\text{Oct})_2$  solution (0.016 mmol) was loaded into a syringe. Promptly, the catalyst and initiator solutions were added to the flask, which was immediately lowered into the oil bath. In a clean scintillation vial,  $\text{ME}_3\text{CL}$  (0.48 g, 1.7 mmol) was placed under vacuum for 2 hours. Meanwhile, the reaction was monitored by GC/MS and  $^1\text{H}$  NMR to check for residual  $\text{ME}_1\text{CL}$  and CL monomers. Upon consumption of the two monomers (about 4 hours reaction time), the  $\text{ME}_3\text{CL}$  was dissolved in 0.25 mL toluene, and then added to the reaction

vessel, which was allowed to stir overnight at 110 °C. The reaction mixture was removed from heat and dissolved in 2 mL THF, and then was poured into a beaker containing hexane, where it crashed out. The polymer was filtered and dried under vacuum, then analyzed by  $^1\text{H}$  NMR and SEC.  $M_n^{\text{NMR}} = 47.2 \text{ kg mol}^{-1}$ ,  $M_n^{\text{SEC}} = 3.7 \text{ kg mol}^{-1}$ ,  $\text{PDI}^{\text{SEC}} = 2.12$ .  $^1\text{H}$  NMR (500 MHz,  $\text{CDCl}_3$ ):  $\delta_{\text{H}}$  1.38 (dd, 0.22H), 1.65 (m, 0.55H) 1.82 (m, 4.2H), 2.30 (t, 0.22H), 2.39 (t, 2.0H), 3.36 (s, 2.8H), 3.59 (m, 12.2H), 4.06 (t, 0.23H), 4.17 (t, 2.0H), 5.11 (s, 0.013H).

**Synthesis of terpolymers P3 and P4.** The syntheses of **P3** and **P4** followed a similar procedure as for **P2**, but the ratio of  $\text{ME}_3\text{CL} : \text{ME}_1\text{CL} : \text{CL} : \text{initiator}$  was 100 : 80 : 20 : 1 for **P3** and 75 : 80 : 20 : 1 for **P4**. The reaction procedures were otherwise comparable. **P3**:  $M_n^{\text{NMR}} = 40.3 \text{ kg mol}^{-1}$ ,  $M_n^{\text{SEC}} = 4.4 \text{ kg mol}^{-1}$ ,  $\text{PDI}^{\text{SEC}} = 1.95$ .  $^1\text{H}$  NMR (500 MHz,  $\text{CDCl}_3$ ):  $\delta_{\text{H}}$  1.38 (dd, 0.13H), 1.65 (m, 0.39H) 1.82 (m, 4.1H), 2.30 (t, 0.14H), 2.39 (t, 2.0H), 3.36 (s, 2.9H), 3.59 (m, 10.1H), 4.06 (t, 0.14H), 4.17 (t, 2.0H), 5.11 (s, 0.011H). **P4**:  $M_n^{\text{NMR}} = 17.0 \text{ kg mol}^{-1}$ ,  $M_n^{\text{SEC}} = 5.7 \text{ kg mol}^{-1}$ ,  $\text{PDI}^{\text{SEC}} = 1.76$ .  $^1\text{H}$  NMR (500 MHz,  $\text{CDCl}_3$ ):  $\delta_{\text{H}}$  1.38 (dd, 0.44H), 1.63 (m, 0.87H) 1.82 (m, 4.8H), 2.31 (t, 0.39H), 2.40 (t, 2.1H), 3.36 (s, 3.1H), 3.60 (m, 8.3H), 4.07 (t, 0.39H), 4.17 (t, 2.0H), 5.11 (s, 0.029H).

**Copolymerization of  $\text{ME}_1\text{CL}$  and CL.** To demonstrate that neither monomer incorporated into the growing chain preferentially, a copolymerization of  $\text{ME}_1\text{CL}$  and CL was conducted. The reaction was set up in the same manner as for **P2-P4**, but with molar ratio of 50 : 50 : 1 for  $\text{ME}_1\text{CL} : \text{CL} : \text{initiator}$ . Samples were taken periodically and analyzed for monomer conversion and relative incorporation into the growing chain using gas chromatography and  $^1\text{H}$  NMR.

#### Characterization

**Preparation of micelles.** Polymeric micelles of the terpolymers were formed by nanoprecipitation and dialysis. In general, the terpolymer (10 mg) was dissolved in THF (0.5 mL) and added dropwise into 10 mL of deionized water while sonicating. The suspension was transferred to SnakeSkin® dialysis tubing (MWCO 3500 Da) and dialyzed against a minimum of 3000 mL deionized water over a 24 hour period. Finally, the dialysis tube contents were filtered through a Nylon syringe filter (0.45  $\mu\text{m}$  pore size), and a 1 mg/mL solution of polymeric micelles was obtained.

**Preparation of NR-loaded micelles.** NR-loaded micelles were prepared in a similar fashion as the blank ones. In general, the terpolymer (5 mg) was dissolved in THF (0.15 mL) in a small vial. A stock solution of NR in THF (5.0 mg/mL) was prepared, and an aliquot (0.1 mL, 0.5 mg NR) was added to the terpolymer solution. This solution was then added dropwise into 5 mL of deionized water while sonicating. The suspension was filtered through a Nylon syringe filter (0.45  $\mu\text{m}$  pore size) to remove excess NR, then was transferred to dialysis tubing (MWCO 3500 Da) and dialyzed against a minimum of 1500 mL deionized water over a 12 h period. The water was exchanged for phosphate buffered saline (1500 mL, pH 7.4 PBS) and dialysis continued for another 12 h. Finally, the dialysis tube contents were filtered through a Nylon syringe

filter (0.45  $\mu\text{m}$  pore size), and a 1 mg/mL solution of NR-loaded micelles was obtained.

**Preparation of DOX-loaded micelles.** DOX-loaded micelles were prepared in a similar fashion as the blank ones. First, the DOX•HCl was neutralized with 3 equivalents of triethylamine in THF:DMSO 5:1.<sup>14</sup> An aliquot (containing 0.5 mg DOX) of the neutralized DOX solution was added to the terpolymer solution (5 mg in 0.2 mL THF). The DOX-polymer solution was then added dropwise into 5 mL of deionized water while sonicating. The suspension was transferred to dialysis tubing (MWCO 3500 Da) and dialyzed against a minimum of 1500 mL deionized water over a 12 hour period. The water was exchanged for phosphate buffered saline (1500 mL, pH 7.4 PBS 1X) and dialysis continued for another 12 hours. Finally, the dialysis tube contents were filtered through a Nylon syringe filter (0.45  $\mu\text{m}$  pore size), and a 1 mg/mL solution of DOX-loaded micelles was obtained. To determine drug loading capacity (LC) and drug loading efficiency (LE), 500  $\mu\text{L}$  of the micelle suspension was added to 500  $\mu\text{L}$  dimethylsulfoxide (DMSO) and subjected to bath sonication (~20 min) to release the DOX from the micelles. After sonication, the absorbance of the solution at 495 nm was fitted to a pre-established standard curve of DOX in PBS/DMSO.

**Analysis of micelles by dynamic light scattering (DLS).** Aqueous suspensions of polymeric micelles were prepared as described above. Prior to measuring, the micelle suspensions were passed through a 0.45  $\mu\text{m}$  Nylon syringe filter. The micelles (400  $\mu\text{L}$  sample size) were analyzed to determine their hydrodynamic diameters using dynamic light scattering with a Malvern Zetasizer Nano ZS instrument equipped with a He-Ne laser (633 nm) and 173° backscatter detector. For some experiments, particle size was analyzed as a function of temperature using 1 °C intervals with a minimum of 60 seconds equilibration time between measurements.

**Investigation of LCST behavior.** A solution of 0.3 wt% polymer in water was prepared and filtered through a 0.45  $\mu\text{m}$  Nylon syringe filter. The solution was stirred and slowly heated in a thermostat-controlled water bath. The change in % transmittance at 600 nm versus the temperature of the solution was recorded on an Agilent UV/Vis spectrophotometer and plotted in Excel. The temperature at which the % transmittance sharply drops (halfway between the max %T and min %T) was taken as the cloud point.

**Determination of CMC.** The critical micelle concentration was determined using the hydrophobic fluorescent molecule pyrene as a probe. Samples of polymer of varying concentrations were combined with a small amount of pyrene in less than 0.1 mL THF. These solutions were added dropwise into 10 mL of deionized water in a scintillation vial with a small stir bar. The solutions were stirred for a minimum of 3 hours to allow the micelles to assemble as the THF evaporated. The resulting aqueous solutions contained  $10^{-5}$  -  $10^0$  g/L of polymer, and a constant pyrene concentration of  $6.67 \times 10^{-5}$  g/L. Fluorescence spectra of the polymer/pyrene solutions were collected with a Perkin-Elmer LS 50 BL luminescence spectrometer at 25 °C with emission wavelength set at 390 nm.

The ratio of the intensities of the pyrene excitation peaks at 338 nm and 335 nm were recorded and plotted against the log of the polymer concentration ( $[c]$ ). The  $x$  coordinate at the intersection of the two trendlines before and after the abrupt increase in the  $I_{338}/I_{335}$  vs.  $\log[c]$  curve was taken to be the critical micelle concentration. Spekwin32 software was utilized in plotting the fluorescence spectra.

**Demonstration of Polymer Degradability.** **P2**, with the highest initial  $M_n$ , was selected for the biodegradability demonstration. **P2** (10 mg) was dissolved in 2.2 mL of PBS (pH 7.4, DNase-, RNase-, and Protease-Free) and was stirred in a closed container over a thermostatted bath at 37 °C for 5 days. Periodically, samples were extracted from the solution and analyzed by SEC to monitor the change in  $M_n$  from  $t = 0$  days to  $t = 5$  days. The data is plotted as % of initial  $M_n$  versus days spent in the PBS solution at 37 °C.

**Micelle Stability in FBS.** NR-loaded micelles **P3<sup>NR</sup>** were incubated in PBS supplemented with 0%, 5%, 10%, 15%, 20%, and 50% volume fetal bovine serum (FBS). In a biological application, synthetic micelles could be destabilized by proteins adsorbing to their surface, thus probing the micelle stability in protein-containing serum such as FBS is prudent. The fluorescence emission intensity ( $\lambda_{\text{ex}} = 550$  nm,  $\lambda_{\text{em}} = 632$  nm) of the NR-micelles was recorded at desired time points. Plotted are the NR emission intensities, normalized to the initial fluorescence intensity at 0 hours, versus time.

#### Cell Culture

For the biological studies, unless otherwise indicated, HeLa cells (donated by Dr. David Boothman, UT Southwestern) were cultured in growth medium (phenol red free Dulbecco's Modified Eagle Medium (Hyclone), supplemented with 5% fetal bovine serum, FBS) at 37 °C, 5% CO<sub>2</sub>, in a humidified atmosphere. Also used in cell viability and cellular uptake studies were phosphate buffered saline (PBS, pH 7.4, DNase-, RNase-, and Protease-Free), nuclear stain DAPI (4',6-diamidino-2-phenylindole dihydrochloride), and MTT (methylthiazolyldiphenyl-tetrazolium bromide).

**Cell Viability (MTT).** Dialyzed micelle solutions (1 mg/mL in 1X PBS) were serially diluted two-fold to 0.50000 mg/mL, 0.25000 mg/mL, 0.12500 mg/mL, 0.06250 mg/mL, and 0.03125 mg/mL respectively. Twenty-four hours prior to the assay, HeLa cells were seeded 96-well tissue culture plate at a density of 10,000 cells per well, in 100  $\mu\text{L}$  growth medium. Following this initial adhesion period, the medium was replaced with 100  $\mu\text{L}$  fresh, pre-warmed growth medium. The micelle dilutions in 1X PBS (80  $\mu\text{L}$ ) were added via pipette were added as final dose ( $\mu\text{g}$  indicated) in 80  $\mu\text{L}$  PBS into cells cultured in 96-well plates in 200  $\mu\text{L}$  growth media. The empty micelles were incubated in cells for 17 hours, then were washed with PBS for 5 minutes. After washing, MTT (methylthiazolyldiphenyl-tetrazolium bromide) solution in medium (110  $\mu\text{L}$  total volume, 10:1 DMEM complete medium : 5 mg/mL MTT in 1X PBS) was added. The cells were incubated for 4 hours to precipitate formazan. All but 25  $\mu\text{L}$  of solution was removed, and 150  $\mu\text{L}$  of dimethylsulfoxide (DMSO) was added. The absorption at 540 nm was recorded

and normalized to the intensity of the untreated cells ( $N \geq 5$ , +/- standard deviation).

**Uptake of DOX-loaded micelles.** HeLa cells were plated on a 96-well plate at a density of 10,000 cells per well and cultured in 100  $\mu$ L growth media. Before adding DOX-loaded micelles, the old media was removed and replaced with 120  $\mu$ L of fresh media. All micelles were added as final dose ( $\mu$ g indicated) in 80  $\mu$ L PBS into cells. The cells were incubated at 37 °C for 4 hours, then washed in PBS, and then incubated for another 24 hours. After fixation (4% PFA for 15 minutes at room temperature followed by washing twice with PBS for 5 minutes PBS) and DAPI staining, 300 nM DAPI in 1X PBS, for 15 minutes at room temperature followed by washing twice with PBS for 5 minutes) the cells were imaged on a BioTek Cytation3 Cell Imaging Multi-Mode Reader.

## Conclusions

Newly synthesized caprolactone-based  $\text{PME}_3\text{CL-}b\text{-P}(\text{ME}_1\text{CL-co-CL})$  terpolymers featured a rare combination of attractive properties: thermoresponsive behavior, biodegradable backbones, and enhanced drug loading capacities. This series of amphiphilic block copolymers exhibited low critical micelle concentrations due to the incorporation of unsubstituted caprolactone into the hydrophobic block, as well as the repositioning of the benzyl end group from the hydrophilic chain end to the hydrophobic end. The terpolymer micelles were loaded with up to 4.97 wt% doxorubicin drug, more than double the amount of previously reported  $\text{PME}_3\text{CL-}b\text{-P}(\text{ME}_1\text{CL-co-CL})$  block copolymers with alkoxy-substituted caprolactone cores. To conclude,  $\text{PME}_3\text{CL-}b\text{-P}(\text{ME}_1\text{CL-co-CL})$  block copolymers demonstrate the synthetic versatility of thermoresponsive  $\text{PME}_3\text{CL-}b\text{-P}(\text{ME}_1\text{CL-co-CL})$  materials and underscore their promising potential in drug carrier applications.

## Acknowledgements

M.C.S. gratefully acknowledges financial support from the Welch Foundation (AT1740), and National Science Foundation (DMR-0956116 & CHE-1126177). D.J.S. gratefully acknowledges financial support from the Welch Foundation (I-1855) and CPRIT (R1212 and RP140110).

## Notes and references

<sup>a</sup> Department of Chemistry, University of Texas at Dallas, Richardson TX, USA.

<sup>b</sup> Department of Biochemistry, University of Texas Southwestern Medical Center, Simmons Comprehensive Cancer Center, Dallas TX, USA.

\*Corresponding author e-mails: (M.C.S.) mihaela@utdallas.edu; (D.J.S.) daniel.sieglwart@utsouthwestern.edu

† Electronic Supplementary Information (ESI) available: [Additional figures]. See DOI: 10.1039/c000000x/

- B. Chertok, M. J. Webber, M. D. Succi and R. Langer, *Mol. Pharmaceutics*, 2013, **10**, 3531-3543.
- M. Elsbahy and K. L. Wooley, *Chem. Soc. Rev.*, 2012, **41**, 2545-2561.
- J. Hao, Y. Cheng, R. J. K. U. Ranatunga, S. Senevirathne, M. C. Biewer, S. O. Nielsen, Q. Wang and M. C. Stefan, *Macromolecules*, 2013, **46**, 4829-4838.
- D. Roy, W. L. A. Brooks and B. S. Sumerlin, *Chem. Soc. Rev.*, 2013, **42**, 7214-7243.
- H. Seyednejad, A. H. Ghassemi, C. F. van Nostrum, T. Vermonden and W. E. Hennink, *J. Control. Release*, 2011, **152**, 168-176.
- J. Hao, E. A. Rainbolt, K. Washington, M. C. Biewer and M. C. Stefan, *Curr. Org. Chem.*, 2013, **17**, 930-942.
- Y. Xiao, M. Yuan, J. Zhang, J. Yan and M. Lang, *Curr. Top. Med. Chem.*, 2014, **14**, 781-818.
- L. Chang, L. Deng, W. Wang, Z. Lv, F. Hu, A. Dong and J. Zhang, *Biomacromolecules*, 2012, **13**, 3301-3310.
- B. Surnar and M. Jayakannan, *Biomacromolecules*, 2013, **14**, 4377-4387.
- A. Mahmud, S. Patel, O. Molavi, P. Choi, J. Samuel and A. Lavasanifar, *Biomacromolecules*, 2009, **10**, 471-478.
- K. Yao, J. Wang, W. Zhang, J. S. Lee, C. Wang, F. Chu, X. He and C. Tang, *Biomacromolecules*, 2011, **12**, 2171-2177.
- J. S. Katz, K. A. Eisenbrown, E. D. Johnston, N. P. Kamat, J. Rawson, M. J. Therien, J. A. Burdick and D. A. Hammer, *Soft Matter*, 2012, **8**, 10853-10862.
- J. Hao, J. Servello, P. Sista, M. C. Biewer and M. C. Stefan, *J. Mater. Chem.*, 2011, **21**, 10623-10628.
- Y. Cheng, J. Hao, L. A. Lee, M. C. Biewer, Q. Wang and M. C. Stefan, *Biomacromolecules*, 2012, **13**, 2163-2173.
- E. A. Rainbolt, K. E. Washington, M. C. Biewer and M. C. Stefan, *J. Mater. Chem. B*, 2013, **1**, 6532-6537.
- H. Maeda, *Adv. Enzyme Regul.*, 2001, **41**, 189-207.
- M. Nichifor, G. Mocanu and M. C. Stanciu, *Carbohydr. Polym.*, 2014, **110**, 209-218.
- P. Kujawa, F. Segui, S. Shaban, C. Diab, Y. Okada, F. Tanaka and F. M. Winnik, *Macromolecules*, 2005, **39**, 341-348.
- M. Nakayama and T. Okano, *Biomacromolecules*, 2005, **6**, 2320-2327.
- Y. Xia, N. A. D. Burke and H. D. H. Stover, *Macromolecules*, 2006, **39**, 2275-2283.
- P. J. Roth, F. D. Jochum, F. R. Forst, R. Zentel and P. Theato, *Macromolecules*, 2010, **43**, 4638-4645.
- T. Mori, Y. Shiota, K. Minagawa and M. Tanaka, *J. Polym. Sci., Part A: Polym. Chem.*, 2005, **43**, 1007-1013.
- V. Torchilin, ed., *Multifunctional Pharmaceutical Nanocarriers*, Springer Science, New York, 2008.
- B. Parrish, R. B. Breitenkamp and T. Emrick, *J. Am. Chem. Soc.*, 2005, **127**, 7404-7410.
- D. Yu, N. Vladimirov and J. M. J. Frechet, *Macromolecules*, 1999, **32**, 5186-5192.
- Z. Ahmad, A. Shah, M. Siddiq and H.-B. Kraatz, *RSC Adv.*, 2014, **4**, 17028-17038.
- Z. L. Tyrrell, Y. Shen and M. Radosz, *Prog. Polym. Sci.*, 2010, **35**, 1128-1143.
- S. Kim, Y. Shi, J. Y. Kim, K. Park and J.-X. Cheng, *Exp. Opin. Drug Deliv.*, 2010, **7**, 49-62.
- X. Shuai, H. Ai, N. Nasongkla, S. Kim and J. Gao, *J. Control. Release*, 2004, **98**, 415-426.

30. Z. Yu, X. ChunSheng, L. MingQiang, D. JianXun, Y. ChenGuang, Z. XiuLi and C. XueSi, *Sci.China Chem.*, 2014, **57**, 624–632.
31. H. Wang, F. Xu, Y. Wang, X. Liu, Q. Jin and J. Ji, *Polym. Chem.*, 2013, **4**, 3012-3019.
32. G. R. Castro, B. K. Larson, B. Panilaitis and D. L. Kaplan, *Appl. Microbiol. Biotechnol.*, 2005, **67**, 767-770.